

Figure S1. NP309-specific memory CD4⁺ T lymphocytes have a CD127^{hi} Sca1^{hi} Bcl2^{hi} phenotype. (A) The representative dot plots show NP309 tetramer binding in CD44^{hi} CD62L^{lo} CD4⁺ T lymphocytes from uninfected versus LCMV-infected mice while the bar graph indicates the number (mean \pm S.D.) of NP309-tetramer⁺ cells in each group (n=5 mice). (B) Dot plots showing CD127 and Sca1 expression in the indicated cell populations as well as a bar graph depicting the frequency (mean \pm S.D.) of each subpopulation among the same populations are displayed (n=5 mice). (C) The representative dot plots show CD127, Sca1, and Bcl2 expression in the indicated cell populations from uninfected and LCMV-infected animals while the bar graph indicates the frequency (mean \pm S.D.) of Bcl2^{hi} fraction among CD127^{hi} Sca1^{hi} cells from the same populations (n=3-4 mice). Data are representative of 2 independent experiments performed. ** $p < 0.01$, *** $p < 0.001$.

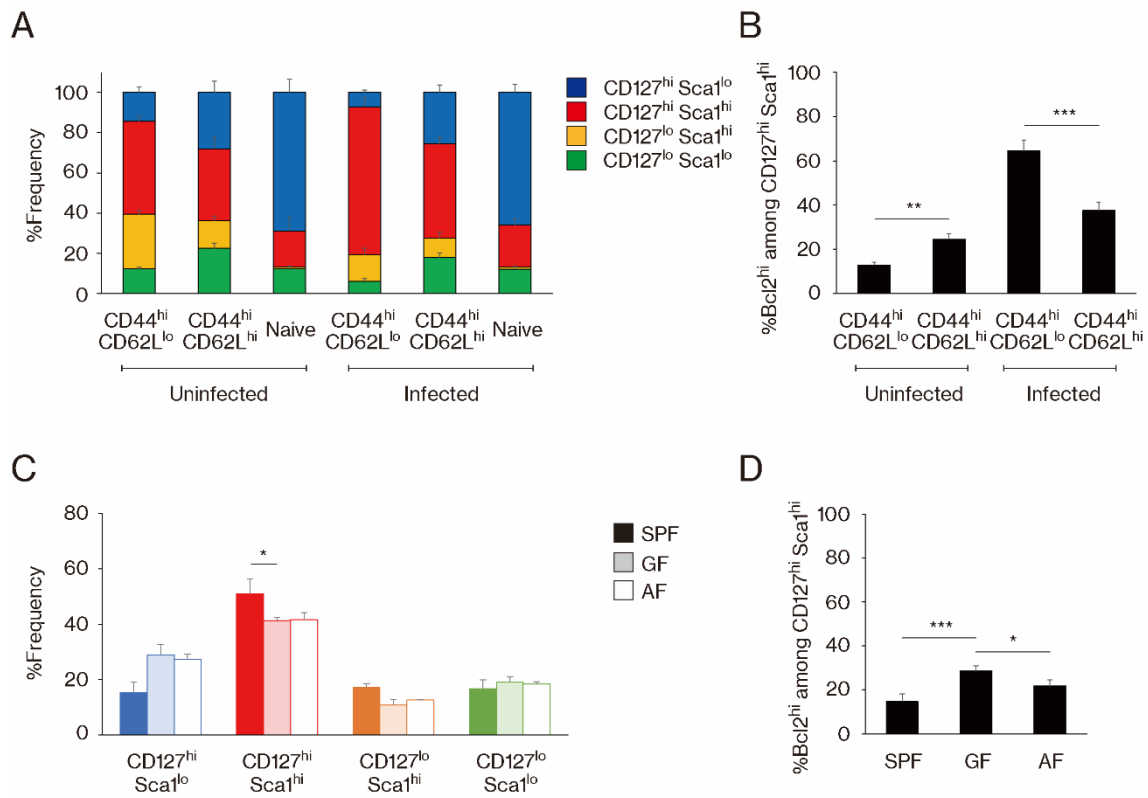


Figure S2. CD44^{hi} CD62L^{hi} CD4⁺ T lymphocytes in uninfected SPF, GF, AF, and LCMV-infected mice. (A) The bar graph shows the frequency (mean \pm S.D.) of CD127^{hi} Sca1^{lo}, CD127^{hi} Sca1^{hi}, CD127^{lo} Sca1^{hi}, and CD127^{lo} Sca1^{lo} cells among the indicated CD4⁺ T cell populations from uninfected SPF and infected mice (n=5 mice). **(B)** The bar graph indicates the Bcl2^{hi} fraction (mean \pm S.D.) among CD127^{hi} Sca1^{hi} cells from CD44^{hi} CD62L^{lo} and CD44^{hi} CD62L^{hi} CD4⁺ T cells in uninfected and LCMV-infected mice (n=3-4 mice). **(C)** The frequency (mean \pm S.D.) of the indicated subsets among total CD44^{hi} CD62L^{hi} CD4⁺ T lymphocytes from SPF, GF, and AF mice (n=3-4 mice). **(D)** The Bcl2^{hi} fraction (mean \pm S.D.) among CD127^{hi} Sca1^{hi} CD44^{hi} CD62L^{hi} CD4⁺ T cells from SPF, GF, and AF animals (n=3-4 mice). Data are representative of 2 independent experiments performed. * $p < 0.05$, ** $p < 0.01$, *** $p < 0.001$.

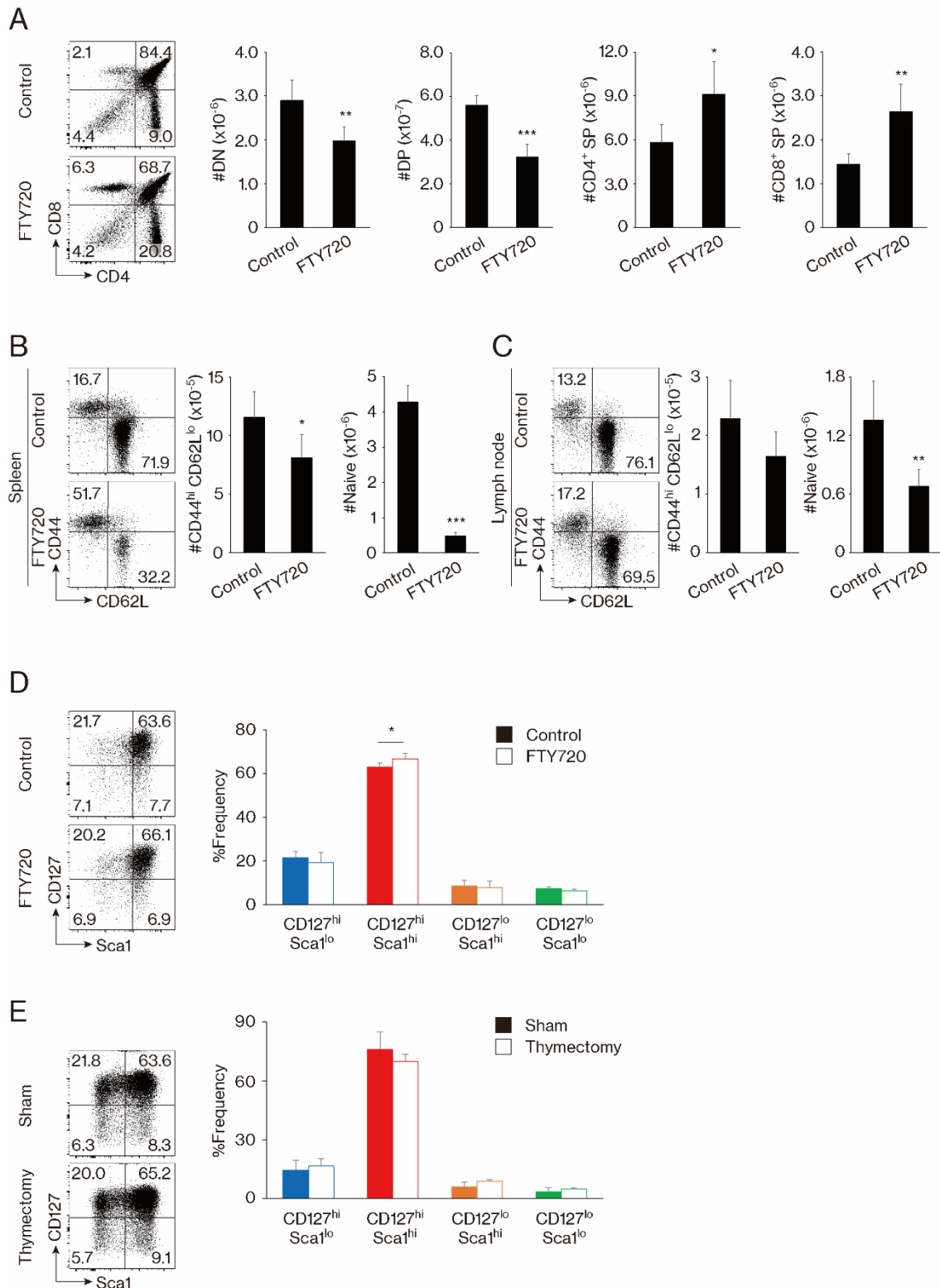


Figure S3. The four MP subpopulations in the periphery are maintained in the absence of thymic input. (A – D) Mice received FTY720 or control PBS and were

analyzed 2 weeks later. (A) Dot plots showing CD4 and CD8 expression in thymocytes from each group together with bar graphs indicating the number (mean \pm S.D.) of double-negative (DN), double-positive (DP), and CD4⁺ and CD8⁺ single-positive (SP) thymocytes (n=5 mice). (B, C) Dot plots displaying CD44 and CD62L expression in CD4⁺ T lymphocytes in the (B) spleen and (C) lymph nodes as well as bar graphs depicting the number (mean \pm S.D.) of MP and naïve cells from each group (n=5 mice). (D) Dot plots showing CD127 and Sca1 levels in splenic MP CD4⁺ T lymphocytes from each group and a bar graph indicating the frequency (mean \pm S.D.) of MP subpopulations among the total MP population (n=5 mice). Data are representative of 2 independent experiments. (E) Mice underwent adult-thymectomy or sham-operation and were analyzed for their MP T lymphocytes 2 weeks later. The representative dot plots display CD127 and Sca1 expression in MP cells from each group while the bar graph indicates the frequency (mean \pm S.D.) of MP subpopulations among total MP cells (n=4 mice). Data are pooled from 3 independent experiments performed. * $p < 0.05$, ** $p < 0.01$, *** $p < 0.001$.

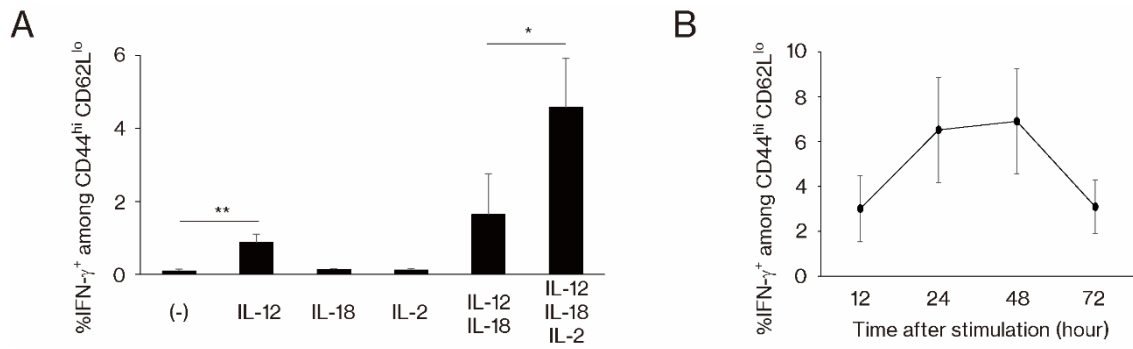


Figure S4. MP cells respond to IL-12, IL-18, and IL-2 and produce IFN- γ . Total splenocytes were cultured **(A)** under the indicated conditions for 24 hours or **(B)** in the presence of IL-12, IL-18, and IL-2 for the indicated period. The graphs indicate the frequency (mean \pm S.D.) of IFN- γ^+ cells among MP CD4⁺ T lymphocytes (n=4 mice). Data are representative of 2 independent experiments. * $p < 0.05$, ** $p < 0.01$.

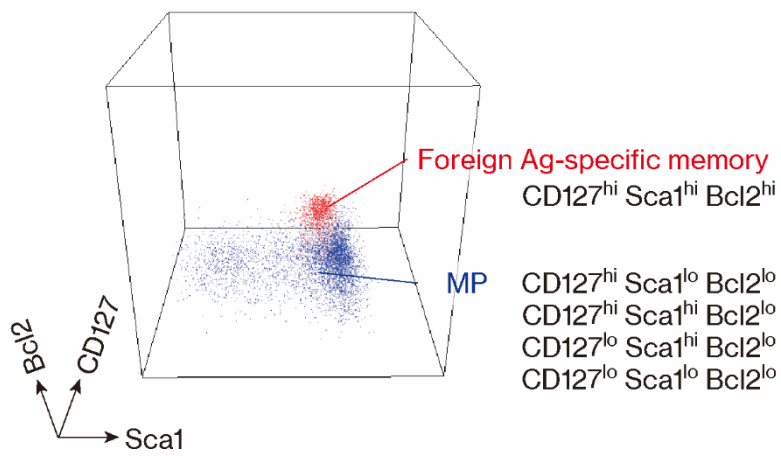


Figure S5. Foreign Ag-specific and MP $CD4^+$ T cells represent phenotypically distinct populations. Foreign Ag-specific memory cells are $CD127^{hi} Sca1^{hi} Bcl2^{hi}$ (red) while MP cells are $CD127^{lo-hi} Sca1^{lo-hi} Bcl2^{lo}$ (blue). Among the latter, $CD127^{hi} Sca1^{hi}$ cells represent the most mature MP subset with the Th1-type inflammatory potential.

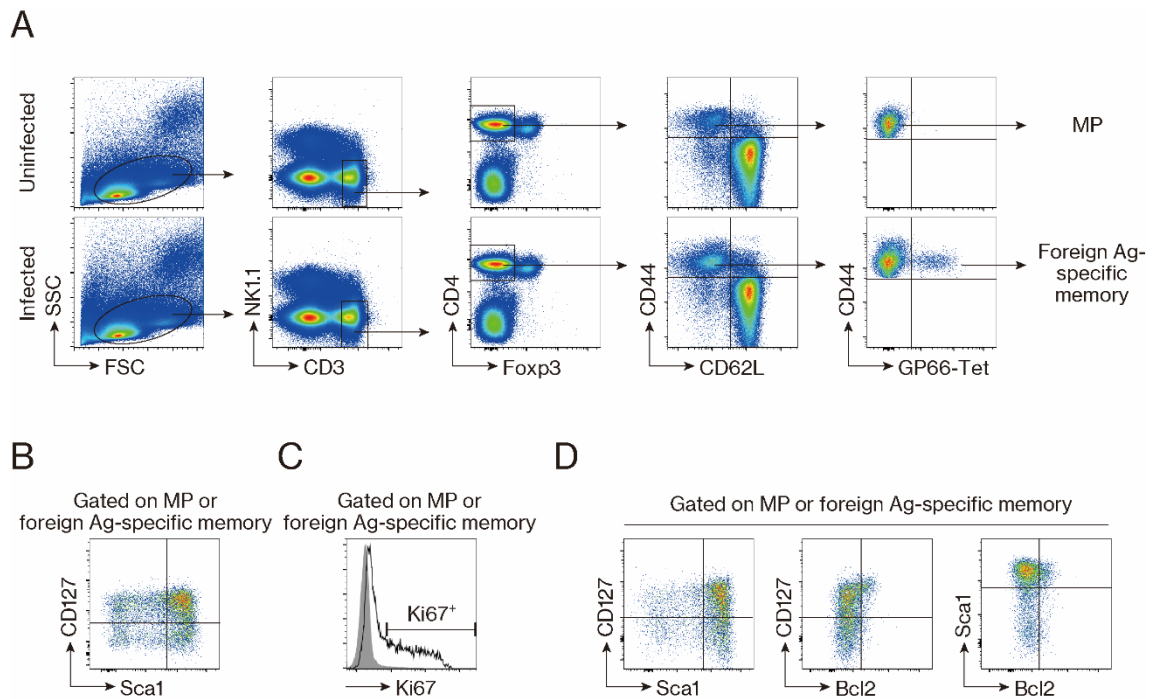


Figure S6. Gating strategy for flow cytometric analyses. (A) To detect MP and foreign Ag-specific memory $CD4^+$ T cells, total singlet cells were gated for $CD3^+$ $NK1.1^{neg}$ $CD4^+$ $Foxp3^{neg}$ $CD44^{hi}$ $CD62L^{lo}$ population. MP and foreign Ag-specific memory cells were then defined as tetramer^{neg} cells from uninfected mice and tetramer⁺ cells from LCMV-infected mice, respectively. (B) To analyze MP subsets, CD127 and Sca1 expression levels were measured in MP or foreign Ag-specific memory cells determined in (A). (C) For examination of proliferation status, Ki67 levels were measured in MP subsets as well as foreign Ag-specific memory cells using naïve cell population as a reference. (D) For detection of Bcl2, CD127, Sca1, and Bcl2 levels were simultaneously analyzed in MP and foreign Ag-specific memory cells. Bcl2^{hi} fraction was determined as the frequency of Bcl2^{hi} cells among CD127^{hi} Sca1^{hi} MP or foreign Ag-specific memory T lymphocyte populations.

Cell cycle (positive regulators)	Cell cycle (negative regulators)	Anti-apoptosis
<i>Aurka</i>	<i>Cdkn1a</i>	<i>Bcl2</i>
<i>Aurkb</i>	<i>Cdkn1b</i>	<i>Bcl2a1</i>
<i>Ccna2</i>	<i>Cdkn2a</i>	<i>Bcl2l1</i>
<i>Ccnb1</i>	<i>Cdkn2b</i>	<i>Bcl2l2</i>
<i>Ccnb2</i>	<i>Cdkn2c</i>	<i>Bcl2l10</i>
<i>Ccnd1</i>	<i>Cdkn2d</i>	<i>Mcl1</i>
<i>Ccnd2</i>	<i>Chek1</i>	<i>Naip1</i>
<i>Ccnd3</i>	<i>Chek2</i>	<i>Naip2</i>
<i>Ccne1</i>	<i>E2f4</i>	<i>Naip3</i>
<i>Cdc25a</i>	<i>E2f5</i>	<i>Naip4</i>
<i>Cdc25b</i>	<i>E2f6</i>	<i>Naip5</i>
<i>Cdc25c</i>	<i>E2f7</i>	<i>Naip6</i>
<i>Cdk1</i>	<i>E2f8</i>	<i>Naip7</i>
<i>Cdk2</i>	<i>Rb1</i>	
<i>Cdk4</i>	<i>Trp53</i>	
<i>Cdk6</i>	<i>Wee1</i>	
<i>E2f1</i>		
<i>E2f2</i>		
<i>E2f3</i>		
<i>Mdm2</i>		
<i>Plk1</i>		
<i>Plk3</i>		
<i>Plk4</i>		
<i>Tfdp1</i>		
<i>Tfdp2</i>		

Table S1. T cell gene signatures.